



Technical Report

RFID Tag Capable of Efficient Free-Space and Near-Metal Operation

Mutharasu Sivakumar and Daniel D. Deavours

ITTC-FY2008-TR-48006-01

February 2008

Project Sponsor:
Kansas Technology Enterprise Corporation

RFID Tag Capable of Efficient Free-Space and Near-Metal Operation

Mutharasu Sivakumar and Daniel D. Deavours

Abstract

The great majority of commercial UHF RFID tags are based on dipole antennas, and it is well-known that the tag performance degrades significantly when placed near a conducting surface. The question we address in this paper is: *is it necessarily so?* In this paper, we present evidence that suggest that it is not, at least to the degree that it has been observed. We present two antennas: one that performs optimally in free-space and performs 15 dB better near metal than a comparable peer. The second antenna is nearly optimal near metal, but operates efficiently over a narrow frequency, and is “good” in free space. We present detailed simulated and measured results for these two tags.

I. INTRODUCTION

Several independent researchers have verified a classic problem: the performance of passive UHF RFID tags degrade when they are close to metal [1], [2], [3], [4]. This is an unfortunate situation, since industry continues to seek a low-cost way to tag metal assets. Microstrip-based antennas (e.g., [5], [6], [7], [8]) offer a useful alternative, but they are usually considerably more expensive. Often, industry simply provides a thin (3 to 6 mm) low dielectric material (foam) in order to provide enough separation from the metal surface to allow for adequate performance. Separations by 3mm often result in a large reduction in overall performance; the best tags are reduced by 16 dB or more over their free-space performance, reducing the read distance by about 85%.

The experiential evidence of this phenomenon is almost overwhelming, leading many to form the working hypothesis:

This work was supported by the Information and Telecommunications Technology Center.

M Sivakumar and D. Deavours are with the Information and Telecommunications Technology Center, University of Kansas, Lawrence, KS 66045, USA. email: {muthus, deavours}@ittc.ku.edu

An RFID tag cannot be designed to simultaneously operate efficiently in free space and near a conducting surface.

While we are unaware that anyone has explicitly claimed this hypothesis, researchers and industry behave as if it is inevitably true. If so, it is a disappointing result, since it would continue to force industry to choose between high-cost and high-performance or low-cost and low-performance solutions. It is certainly desirable to use a tag designed for operation in free-space (the majority of use cases) where economies of scale can drive costs low, and also be able to apply an inexpensive, thin foam backing material, and use that same tag for tagging metal assets and achieve similar performance. As we describe in Section II-A, high-speed converting equipment exists that rapidly and inexpensively manufacture these tags.

Fortunately, the working hypothesis is false. In this paper, we describe two antenna designs that operate at relatively high levels of performance both in free space and near metal. These antennas are not optimal, but they are good enough to prove 15 to 20 dB on-metal performance improvement over comparable commodity tags. Both antennas are designed to be converted with a 3.18 mm HDPE foam spacer. The first antenna is designed to operate optimally in free-space (2 dBi) and relatively mildly degraded (-2 dBi) with a 3.18 mm foam spacer from a copper plate. The second antenna was designed to present a near-optimal impedance match on metal (3 dBi), but suffers from a free-space effective gain of -6 dBi. We do not claim these antenna designs are “optimal” solution, but rather as conclusive evidence that antennas can be developed to operate much more efficiently in two different environments than any known commercial tag. We give extensive free-space and on-metal performance results for both tags. We conclude with some observations and future work.

II. BACKGROUND

A. *Manufacturing of RFID Tags*

There are a number of ways in which RFID tags can be manufactured. We present one (simplified) method that is commonly employed for illustration.

UHF RFID tags are commonly manufactured using a web-based process, i.e., “roll-to-roll.” Commonly, antennas are printed, deposited, or etched on a PET film that provides dimensional stability. (Printing to paper is also possible, as are a number of other techniques.) Next, a high-speed flip-chip assembly or strap-attach machine rapidly affixes the RFID IC to the antenna. The



Fig. 1. Commercial example of a commodity tag with 4.76 mm foam backing.

roll is then slit and wound into rolls, which is called the “dry inlay.” One possible next step is that inlay can be converted by applying a pressure-sensitive adhesive (PSA), die cut, and placed on a release liner, which results in a “wet inlay.” From the wet inlay, one can attach the inlay to a label stock, die cut the label, and place on a release liner, which is called a “smart label.” Smart labels can then be printed, the RFID tag encoded, and applied using label applicators.

The label stock is a paper or film that comes as a continuous roll with a PSA and release liner. When the inlay is being converted to a label, first, the label stock is delaminated, i.e., the label stock is separated from the release liner. The wet inlay is transferred onto the label stock at the proper location. Next, the label stock and release liner are re-laminated (brought back together), the label is die cut, and the waste is removed. Converting machine speeds vary, but 20,000 units per hour is typical.

It is relatively straightforward to modify the conversion process to incorporate a foam backing. When the label is re-laminated, instead of re-laminating to the release liner, one can laminate the label to a foam “tape,” which includes the foam material, PSA, and release liner. The resulting stack can then be die cut as usual. (See Figure 1 for a commercial example.) This can be done with a minimal impact on conversion speeds, with modest additional material costs, and with minimal modifications to expensive conversion machines. This is one reason why foam-backed tags are popular and inexpensive.

B. Performance of Commodity RFID Tags

To illustrate how RFID tags degrade when placed near metal, we performed the following experiment. We placed tags in free space, directly on metal, and separate the tag from metal by 1/16, 1/8, 3/16, and 1/4 inch white HDPE foam with density of six pounds. We placed the tags on a metal plate approximately 22cm by 28 cm. We then measured the maximum distance that the tag was detectable by a ThingMagic Mercury4 reader at full power using bistatic, circularly-

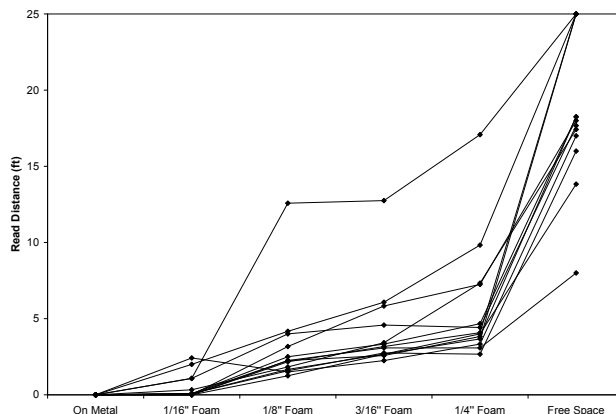


Fig. 2. Various tag read distance vs. foam separation from metal.

polarized antennas. We placed anechoic cones on the floor to eliminate the ground multi-path. Figure 2 shows the results of 13 ISO 18000-6c (EPC “Gen 2”) tags from five vendors.

It should be noted that the sole outlier is a tag that is a large, “dual dipole” tag with an antenna of approximately 100 mm by 100 mm form factor. The dual dipole antenna reduces the polarization mismatch between circularly-polarized reader antenna and linear polarization of most tag antennas (i.e., improving the tag performance by 3 dB). The larger form factor also makes it expensive to manufacture and convert, as well as bulky to deploy.

Removing that outlier, it is clear that nearly all tag antennas degrade significantly and similarly when near a metal ground plane. All other tags closely follow a relatively narrow performance envelope, with performance reducing as the separation reduces. We observed that industry uses between 0.125 inch (3.18 mm) and 0.25 inch (6.35 mm) foam separation. Performance at 3.18 mm may be usable for some applications, but provides drastically reduced performance. Performance with the 6.35 mm foam separation is more practical for many applications, but it is clear from Figure 2 that the performance is still significantly degraded from its free-space performance.

Data from another experiment [3] shows similar results. Here, the same reader and antennas were used, but we attenuated the reader transmit power to simulate distance, and used the Friis equation (see Section II-D) to estimate the read distance. Here, the tag was placed on a rigid expanded polystyrene foam block, with the foam interposed between the tag and reader. Thus, only air separated the tag from the metal surface. The tag was separated by various distances

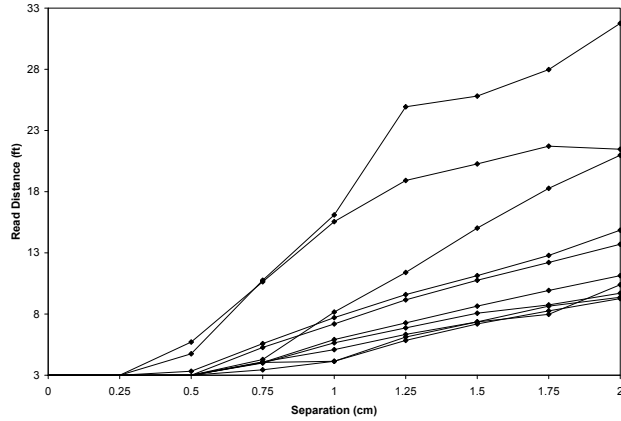


Fig. 3. Various tag read distance vs. air separation from metal.

from the metal surface, and the reader power attenuated until the tag was unreadable. Figure 3 shows the results of 10 “Gen 1” RFID tags from three vendors. The results are again very consistent with the previous experiment. Again, the three best-performing tags used a different and more efficient IC, so we see two clearly-defined performance bands.

Others have reported very similar results [1]. It is this preponderance of evidence that has led practitioners to the working hypothesis: *RFID tags near metal degrade according to a fairly well-defined performance envelope*. The result has been relatively little effort to develop antennas that will operate outside of this envelope.

C. Other Near-Metal Tags

A notable exception to the dipole and microstrip antennas is the work of [9], which presents an antenna designed to work on a foil-lined package. This antenna is a hybrid-type antenna using microstrip-like features. This antenna was designed for tagging a particular item with a unique geometry and electrical characteristics, so it is not clear if the antenna will generalize. The performance results are a disappointing 0.5 meters of read distance using circularly-polarized antennas, and has an impractical size for general application, being 271 mm long. However, [9] provides performance in both 865–868 and 902–928 MHz frequency bands, while the antennas we present here focus solely on operation in the 902–928 MHz band.

D. Tag Performance Metrics

The performance of an antenna is often defined by its *gain*, G , which is the product of the directivity, D , and efficiency, η . Directivity is further defined as

$$D(\theta, \phi) = \frac{U(\theta, \phi)}{U_0}$$

where $U(\theta, \phi)$ is the radiation intensity in the (θ, ϕ) direction, and U_0 is the average radiation intensity, or the total radiated power divided by 4π . For convenience, we often write D to mean the maximum directivity.

Efficiency is the ratio of energy radiated to the total energy entering the antenna. Sources of losses include resistive losses (due to imperfect conductors) or dielectric loss (materials converting electric fields into heat). Gain defines one aspect of antenna efficiency, but that alone is insufficient for describing RFID tags.

One critical aspect of tag performance is the degree of coupling between the antenna and the IC. If the IC has an impedance of Z_c and the antenna presents an impedance of Z_a , maximum power is transferred between tag and antenna when $Z_a = Z_c^*$, i.e., the complex conjugate. The fraction of power transferred to the maximum possible transferred is given by [10], [11]

$$\tau = \frac{4R_a R_c}{|Z_a + Z_c|^2}.$$

Similarly, a *power wave reflection* can be defined as

$$s = \frac{Z_c - Z_a^*}{Z_a + Z_c},$$

so that $\tau + |s|^2 = 1$. Here, s plays a similar role to S_{11} in the traditional antenna matching problem. We can define a Smith chart transformation

$$\hat{z}_a = r + jx = \frac{R_a}{R_c} + j \frac{X_a + X_c}{R_c}.$$

so that $\hat{z}_a = \frac{1+s}{1-s}$. This allows us to plot \hat{z}_a on a Smith chart.

Finally, the free-space Friis equation can be modified for RFID transponders [12].

$$r = \frac{\lambda}{4\pi} \sqrt{\frac{P_t G_t G_r \tau \rho}{P_{th}}}$$

We follow the convention of [12] that the subscript t represents the transmitter (reader) and the subscript r represents the receiver (tag); τ is the power transfer efficiency, ρ is the polarization mismatch, and P_{th} is the minimum (threshold) power to operate the IC. Commonly, readers use

circularly polarized antennas and tags use linearly polarized ones, leading to a polarization loss of 50%. We can write a term that combines all the tag-dependent factors as $D\eta\tau/P_{th}$ with units Watts^{-1} . If we ignore the power efficiency of the IC, we can measure the quality of the tag antenna using a modified gain term $G_{eff} = D\eta\tau$, which we call *effective gain*.

III. ANTENNA DESIGN

The process of developing RFID dipole antennas has been presented elsewhere [13], [14]. The antennas we present here are not substantially different from those developed in the literature except for two factors. First, we tend to use wider striplines for the antenna element than is common. Wide striplines are used to reduce the conductive losses when the tag is close to metal and operates like a microstrip antenna. Second, we use relatively wide striplines in forming the inductive arms of the matching circuit. This plays an important role in finding the balance between efficient operation in free-space and on-metal.

Both antennas were designed to be converted with a 3.18 mm HDPE foam spacer with a six pound density, which we estimate from measurements to have a dielectric constant of 1.09 and loss tangent of 0.0015. (The HDPE foam is cross-linked, which is why a six pound HDPE foam has such a high loss tangent.)

We developed two antennas for two different objectives. The first antenna was designed to be optimized for free-space performance, and the objective was to see how high we could get the on-metal performance. The second antenna was designed to be optimized for the on-metal performance, and the objective was to see how high we could get the free-space performance.

In free space, the antennas operate like a “normal” RFID dipole antenna. The striplines in the matching circuit behave like inductors, which is typically used to add inductance in order to match to a capacitive IC. When the tag is placed on metal, the antenna behaves like a microstrip antenna using a balanced feed [15]. The striplines used for the matching circuit become microstrip transmission lines, with the width governing the characteristic impedance of the matching circuit. We place the resonant frequency of the antenna behaving as a microstrip at 930 to 960 MHz, so we operate the antenna below resonance where the magnitude of the impedance is lower. The resonant frequency, gap between the feeds, length, and width of the feed striplines are all part of the system that has to be carefully tuned in order to make the antenna work well in both environments. As future work, we would like to develop a detailed model for the antenna in

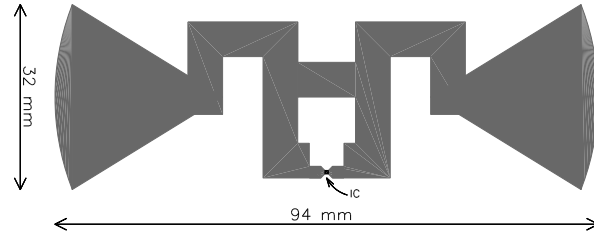


Fig. 4. Antenna 1. The dark area represents the metalized portion of the antenna.

both environments in order to determine performance bounds and develop optimal designs.

A. Antenna 1

Antenna 1 was designed to perform and behave similar to a “normal” RFID tag based on a wide, stripline dipole antenna [16]. Figure 4 illustrates the first antenna with dimensions. The significant difference with this antenna is that we use much wider striplines within the matching circuit than is typically done. Wide striplines reduce the inductance per unit length of a stripline inductor, and reduce the characteristic impedance of a microstrip transmission line.

The antenna was etched from 18 micron copper on a 75 micron PET film. The tags were designed to work with a IC impedance of $12 - j133$ Ohms. We gave ourselves the practical constraint of needing to fit within a form factor of 94 mm by 32 mm, which is the form factor of a popular commodity tag used for a similar purpose. The tag is centered on a 3.18 mm HDPE foam substrate with dimensions 101.6 mm by 38.1 mm (4 inches by 1.5 inches).

Figure 5 presents the impedance of the simulated and measured tag in the free-space environment using a power wave Smith chart normalized to the IC impedance ($12 - j133$ Ohms). We plot the impedance at 5 MHz intervals over the range from 900 MHz to 930 MHz. We used a finite element simulation tool [17] to simulate the tag. To measure, we used a network analyzer and a chip balun mounted on a small PCB to probe the tag at the strap mount points. Note that the impedance has a small resistance and large reactance, and therefore is not likely to be highly accurate. Next, Figure 11 presents the measured and simulated impedance on a copper ground plane with dimensions 22 cm by 28 cm. Both the simulated and measured resonant frequency (peak antenna resistance) was found to be 965 MHz.

We note that the simulated and measured impedance values show generally good agreement.

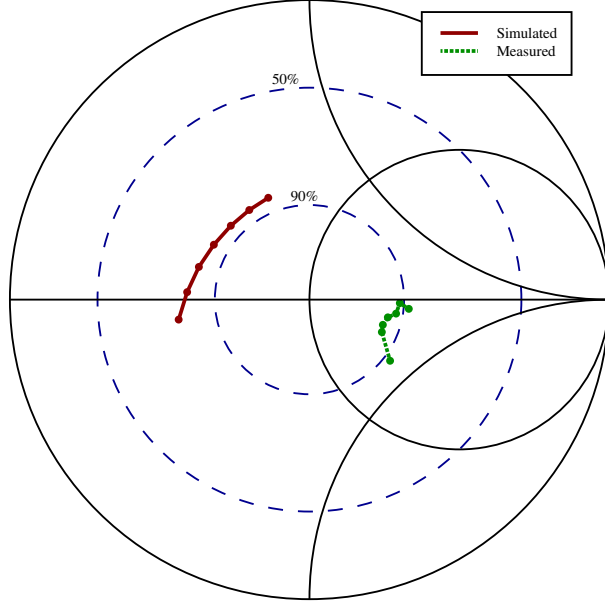


Fig. 5. Smith chart of Antenna 1 simulated and measured impedance in free space, normalized to $12 - j133$ Ohms.

Note that the Smith charts are normalized to $12 - j133$ Ohms, and thus exaggerates small changes in resistance more than a Smith chart normalized to 50 Ohms would. Our measured resistance was consistently larger than the simulated resistance, which we attribute to measurement and calibration error. Generally, the two show good agreement, and the results are sufficiently close to believe that the free-space impedance match is excellent. The impedance on metal is more likely to follow the simulated impedance curve, where there is a 3 dB impedance match loss. However, both simulated and measured reactance is well matched at the center frequency.

Next, we measure the tag performance. To measure tag performance, we placed the tag 2 meters from a Samsys MP-9320 reader using a circularly-polarized monostatic antenna and varied the reader power in 1 dB increments, and found the minimum power in which the tag was detectable. We assume our tag presents an optimal antenna impedance in free space, and note that the tag can be read at 2 meters with the reader power at 13 dBm. From that, we estimate that the IC power requirements are $P_{th} = -16.5$ dBm. Using the modified Friis equation, we can calculate the the effective gain, and compare with the simulated effective gain in Figure 7, for both free-space and on-metal performance. While not shown, we did observe a measured peak G_{eff} in free space of 2 dBi between 915 and 920 MHz.

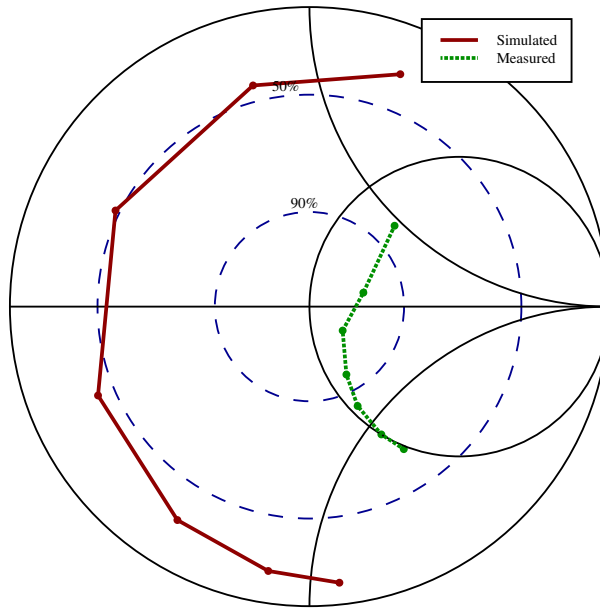


Fig. 6. Smith chart of Antenna 1 simulated and measured impedance on metal, normalized to $12 - j133$ Ohms.

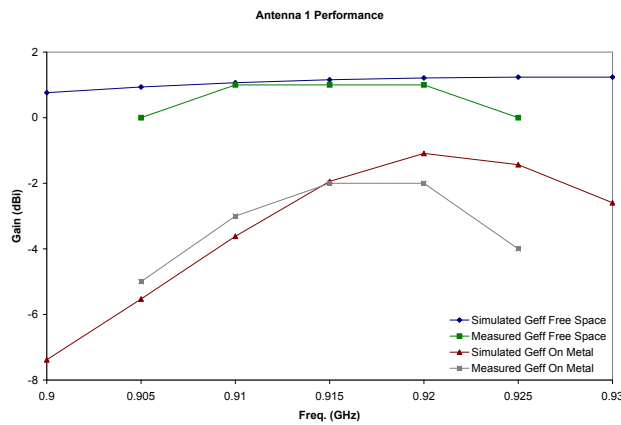


Fig. 7. Smith chart of Antenna 1 simulated and measured performance in free space and on metal.

It should be noted that the on-metal directivity is approximately 8.5 dBi, and the simulated antenna efficiency on metal is -6.5 dB, with approximately half of the losses attributed to conductive loss and half to dielectric loss. So the increase in directivity from free space to on metal is negated by about the same amount of loss. The additional loss comes from a reduction in τ . We see excellent agreement between the predicted and measured performance both in free space and on metal.

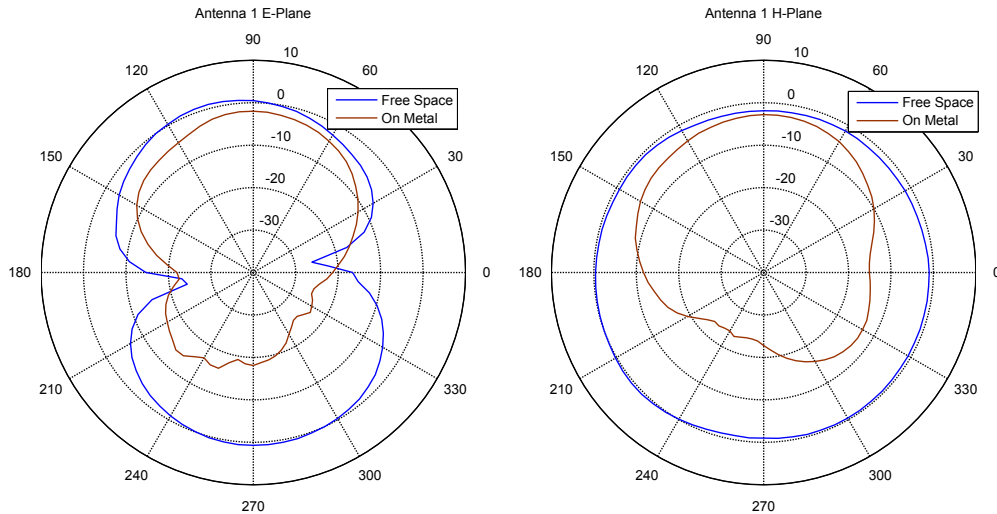


Fig. 8. E- and H-plane radiation pattern in free space and on metal at 915 MHz using G_{eff} .

We measured the radiation pattern of the antennas both in free space and on metal, and present the results in Figure 8. The measurements were taken at 915 MHz, and the directivity pattern was scaled using the peak G_{eff} . Clearly, the antenna becomes more directive on metal, and the on-metal directivity would increase with a larger ground plane.

While the results from Antenna 1 are excellent, we emphasize that this antenna is not necessarily optimal, and future improvements may yield even better antennas. However, it does provide conclusive proof that one can, in fact, design tags that performs nearly optimal in free space and can perform at a relatively high level with a thin foam separation from metal.

B. Antenna 2

Antenna 2 was designed with the opposite objective: achieve the highest level of performance possible on metal, and within that constraint, achieve good free-space performance. We were not as successful with Antenna 2 as with Antenna 1, but it is still instructive to see what is possible.

We begin with an illustration of the antenna design, given in Figure 9. Note that the stripline widths are thicker than Antenna 1 (8 mm vs. 6 mm), which was done to reduce conductive losses. Otherwise, the matching circuit was modified only slightly for the new design constraint.

Figures 10 and 11 show the simulated and measured impedance in free space and on metal, respectively. From Figure 10, we see that the free space impedance is poorly matched. Although

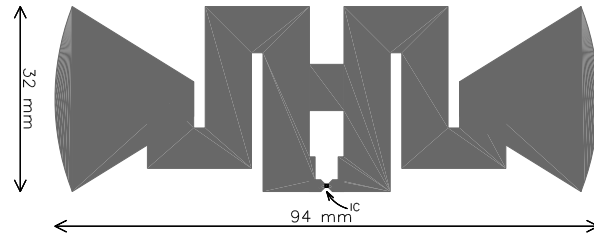


Fig. 9. Antenna 2. The dark area represents the metalized portion of the antenna.

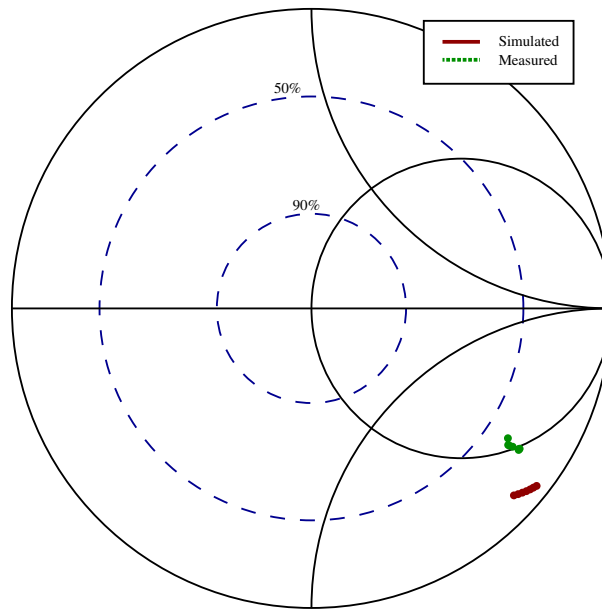


Fig. 10. Smith chart of Antenna 2 simulated and measured impedance in free space, normalized to $12 - j133$ Ohms.

the antenna resistance is good, the antenna presents a load that is not sufficiently inductive. Initial simulation results from a method of moments code indicated a larger free-space reactance, which would have resulted in a substantially improved free-space impedance match. The simulated results in Figure 10 are from a finite element code, and indicate better agreement with measurement, but worse free-space performance than initially anticipated.

The impedance achieved on metal is excellent. The resonant frequency was predicted to be 930 MHz in simulation and measured at 925 MHz, which accounts for the reduced performance at the higher frequencies. We see good agreement between simulated and measured impedance. We can also see that the impedance is changing quite rapidly, and that τ from the measured

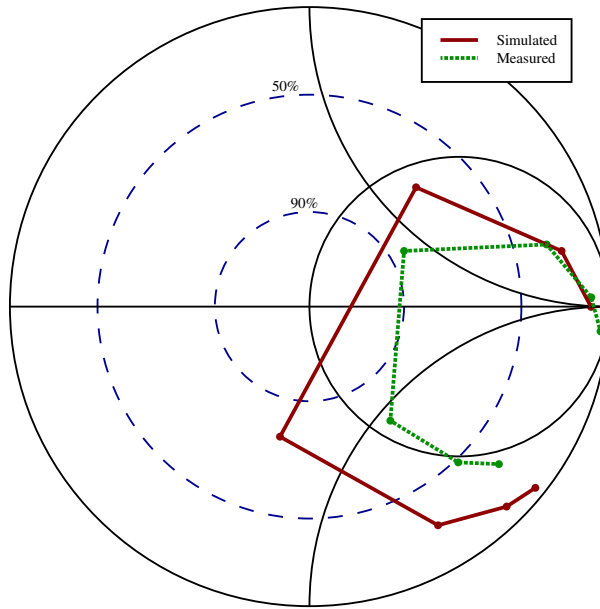


Fig. 11. Smith chart of Antenna 2 simulated and measured impedance on metal, normalized to $12 - j133$ Ohms.

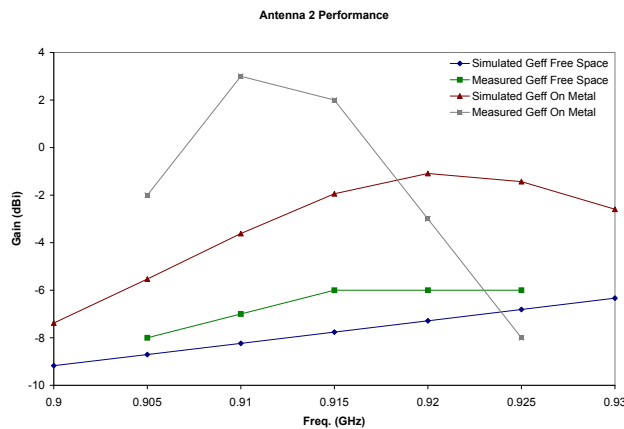


Fig. 12. Antenna 2 simulated and measured performance in free space.

impedance falls off rapidly at the higher frequencies.

The difference between simulated and predicted performance of Antenna 2 in free space is modest. The difference on metal is more substantial, where the measured performance is both higher than expected, likely due to impedance matching better than predicted, and increased efficiency due to operating closer to resonance than predicted. It is also possible that the estimated loss tangent of the substrate is smaller than the value we estimated.

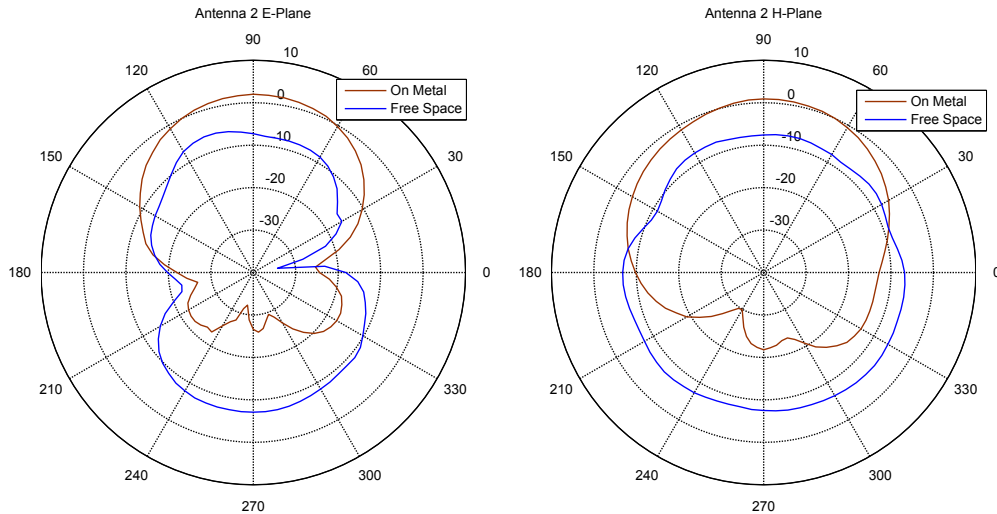


Fig. 13. Radiation pattern of Antenna 2 in free space and on metal at 915 MHz plotting G_{eff} .

The radiation pattern is given in Figure 13, which is substantially similar to that of Antenna 1.

Clearly, Antenna 2 can be improved in a number of ways. Most importantly, the resonant frequency should be moved to a higher frequency, such as 940 to 950 MHz, which will help mitigate the narrow bandwidth. Second, we should increase the free-space reactance, which can substantially improve the free-space performance. We include Antenna 2 not because it is an optimal design, but rather because it directly supports the thesis that it is possible to design tags that perform substantially better in free space and on metal than current RFID tags do. We believe that with additional work, Antenna 2 will be able to have substantially improved free-space performance, perhaps to $G_{\text{eff}} = -3$ or -2 dBi.

C. Comparison

Here, we briefly compare the performance results of the two antennas with the ALN-9540 RFID tag [18]. We chose the ALN-9540 for two reasons. First, we have found it to be one of the better-performing tags near metal with a comparable form factor. The ALN-9540 is 95 mm by 8 mm, and tags that perform marginally better near metal are either approximately 150 mm long or approximately 100 mm square. Second, it uses the same IC as the antenna we constructed, and so it is easier to perform direct comparisons. However, one should use caution

TABLE I
SUMMARY OF COMPARABLE TAG PERFORMANCE.

Foam separation	Peak G_{eff} (dBi)		
	ALN-9540	Antenna 1	Antenna 2
1.59 mm	< 30		
3.18 mm	-17	-2	+3
4.76 mm	-14		
6.35 mm	-10		
Free Space	-1	+2	-6

when performing direct comparisons because two ICs can have slightly different Z_c and different P_{th} . We emphasize that the important results are not the absolute values in the results, but rather the difference between the free-space and 3.18 mm foam on-metal performance. Table I shows the results of the three tags tested. Note the -1 dBi free-space performance for the ALN-9540 may be due to larger P_{th} (and thus the G_{eff} may be as much as 3 dB larger) or because the ALN-9540 antenna presents a imperfect impedance match for other reasons. We observe a 16 dB of difference in performance for the ALN-9540 in free space and on metal with a 3.18 mm foam separation. Antenna 2 has only 9 dB difference, but yields excellent on-metal performance, and Antenna 1 has only 4 dB difference while achieving a near-perfect free-space impedance match.

Practically, let us assume a $P_{\text{th}} = -16.5$ dBm and $\rho = 0.5$. An effective gain of -6 dBi yields a read distance of 3.9 meters, -2 dBi yields 6.2 meters, -1 dBi yields 7.0 meters, $+2$ dBi yields 9.8 meters and $+3$ dBi yields 11.0 meters of read distance.

IV. CONCLUSIONS

In this paper, we present two RFID tag antennas that are designed to work relatively well both in free space and on metal. The first antenna presents 2 dBi of effective gain in free space and -2 dBi on metal (compared to -1 dBi of effective gain from a similar commodity RFID tag in free space). The second presents 3 dBi of effective gain on metal, and -6 dBi in free space. It is likely that minor adjustments to the second antenna can yield substantially improved free-space performance.

More significantly, the results demonstrate that it is possible to develop tags that behave near-optimally in free space and on metal. The performance envelopes shown in Figures 2 and 3 are not how dipole antennas *must* behave. The antennas we present here are presented as evidence. These antennas offer substantially improved performance over commodity antennas, yet it is still possible that substantially better-performing antennas can be developed. Our next steps will be to develop accurate models of the tags in different environments so as to establish performance bounds, and to use those models to develop design methodologies for this new class of antenna.

REFERENCES

- [1] D. M. Dobkins and S. Weigand, "Environmental effects on RFID tag antennas," in *IEEE MTT-S International Microwave Symposium*, Long Beach, CA, June 2005, pp. 4–7.
- [2] J. D. Griffin, G. D. Durgin, A. Haldi, and B. Kippelen, "RF tag antenna performance on various materials using radio link budgets," *Antennas and Wireless Propagation Letters*, vol. 5, no. 1, pp. 247–250, Dec. 2006.
- [3] K. M. Ramakrishnan and D. D. Deavours, "Performance benchmarks for passive UHF RFID tags," in *13th GI/ITG Conference on Measurement, Modeling, and Evaluation of Computer and Communication Systems*, Nuremberg, Germany, Mar. 2006, pp. 137–154.
- [4] S. R. Aroor and D. D. Deavours, "Evaluation of the state of passive UHF RFID: An experimental approach," *IEEE Systems Journal*, vol. 1, no. 2, pp. 168–176, 2007, to appear.
- [5] M. Hirvonen, P. Pursula, K. Jaakkola, and K. L. Laukkanen, "Planar inverted-F antenna for radio frequency identification," *Electronics Letters*, vol. 40, no. 14, pp. 848–850, July 2004.
- [6] L. Ukkonen, L. Sydänheimo, and M. Kivikoski, "A novel tag design using inverted-f antenna for radio frequency identification of metallic objects," in *2004 IEEE/Sarnoff Symposium on Advances in Wired and Wireless Communications*, 2004, pp. 91–94.
- [7] H. Kwon and B. Lee, "Compact slotted planar inverted-F RFID tag mountable on metallic objects," *Electronics Letters*, vol. 41, no. 24, pp. 1308–1310, Nov. 2005.
- [8] H. W. Son, G. Y. Choi, and C. S. Pyo, "Design of wideband RFID tag antenna for metallic surfaces," *Electronics Letters*, vol. 42, no. 5, pp. 263–265, Mar. 2006.
- [9] L. Ukkonen, D. W. Engels, L. Sydänheimo, and M. Kivikoski, "Operability of folded microstrip patch-type tag antenna in the UHF RFID bands within 865–928 MHz," *IEEE Antennas and Wireless Propagation Letters*, vol. 5, pp. 414–417, 2006.
- [10] K. Kurokawa, "Power waves and the scattering matrix," *IEEE Transactions on Microwave Theory and Technique*, vol. 13, no. 3, pp. 194–202, Mar. 1965.
- [11] P. V. Nikitin, K. V. S. Rao, S. F. Lam, V. Pillai, R. Martinez, and H. Heinrich, "Power reflection coefficient analysis for complex impedances in RFID tag design," *IEEE Transactions on Microwave Theory and Technique*, vol. 53, no. 9, pp. 2721–2725, Sept. 2005.
- [12] P. V. Nikitin and K. V. S. Rao, "Reply to 'Comments on "Antenna design for UHF RFID tags: A review and a practical application"'," *IEEE Transactions on Antennas and Propagation*, vol. 54, no. 6, pp. 1906–1908, June 2006.

- [13] K. V. S. Rao, P. V. Nikitin, and S. F. Lam, "Antenna design for UHF RFID tags: A review and a practical application," *IEEE Transactions and Propagation*, vol. 53, no. 12, pp. 3870–3876, Dec. 2005.
- [14] S. S. Serkan, S. Bhattacharya, L. Yang, A. Rida, M. M. Tentzeris, and J. Laskar, "Design of a novel high-efficiency UHF RFID antenna on flexible LCP substrate with high read-range capability," in *Antennas and Propagation Society International Symposium 2006*, 2006, pp. 1031–1034.
- [15] M. Eunni, M. Sivakumar, and D. D. Deavours, "A novel planar microstrip antenna design for UHF RFID," *Journal of Systemics, Cybernetics and Informatics*, vol. 5, no. 1, pp. 6–10, Jan. 2007.
- [16] D. M. Dobkins, *The RF in RFID: Passive UHF RFID in Practice*. Burlington, MA: Newnes, 2007.
- [17] Ansoft Corporation, *HFSS Online Help*, Ansoft Corporation, Pittsburg, PA, 2006.
- [18] Alien Technology, Inc., "Aln-9540 product overview," http://www.alientechnology.com/docs/products/DS_ALN_9540_Squiggle.pdf, Sept. 2007, referenced December 15, 2007.